JOURNAL OF
Materials
CHEMISTRY

An XPS study on the degradation of lead magnesium niobate-based relaxor ferroelectrics during nickel electroplating

JiangLi Cao,* LongTu Li and ZhiLun Gui

State Key Laboratory of New Ceramic and Fine Processing, Department of Materials Science and Engineering, Tsinghua University, Beijing 100084, China. E-mail: perov@sina.com; Fax: +86-10-62771160; Tel: +86-10-62784579

Received 25th August 2000, Accepted 20th December 2000
First published as an Advance Article on the web 28th February 2001

Resistance degradation of $Pb(Mg_{1/3}Nb_{2/3})O_3$–$Pb(Zn_{1/3}Nb_{2/3})O_3$–$PbTiO_3$ (PMZNT) relaxor ferroelectrics during nickel electroplating was investigated by resistivity measurement and X-ray photoelectron spectroscopy (XPS) through the appearance of changes in Nb 3d and Pb 4f spectra. It was found that the insulation resistance of the PMN-based ceramics decreased after electroplating. The XPS analysis showed that the ceramic materials had been reduced by hydrogen during electroplating and Nb^{4+} and metallic Pb were generated. As a result, oxygen vacancies and free electrons were created and, therefore, increased the conductivity of the ferroelectrics. It was also found that Nb^{5+} reduction was prior to Pb^{2+} reduction. On the basis of our experiments, two conduction mechanisms involved in the hydrogen-induced resistance degradation were established.

1 Introduction

Much effort has been dedicated to the manufacturing and properties of lead-containing relaxor perovskite compounds. Amongst them, lead magnesium niobate (PMN) has received much attention and been intensively studied[1–6] owing to its high dielectric constant, broad maximum, high electrostrictive strain coefficient and relatively low firing temperature. PMN-based ceramics have been used on many dielectric and electrostrictive devices.[7–10]

Multilayer ceramic capacitors (MLCC) are widely used in various electronic circuits. Extremely high reliability is required to keep up with development trends. PMN-based ceramics is one of the most important systems for the MLCC excellent performance. However, some properties of PMN perovskite remain unclear. In MLCC fabrication, a three-layer-electrode technique is widely adopted, *i.e.* Ag electrode/Ni coating/Sn–Pb coating. Unfortunately, it was found that nickel and tin plating often had a negative influence on the properties of the MLCC, or sometimes even led to a complete degradation.[11,12] The degradation mechanism of PMN-based ceramics is of much importance with regard to the improvement of reliability of or the design of new materials. Much attention has been paid to this; however, these studies were focused on the ambiguous effects of plating process variables.[13,14] A fundamental understanding about the intrinsic nature of the degradation mechanism is still lacking.

It is well known that hydrogen can be generated during electroplating,[15] and there has been much research towards hydrogen-induced degradation of metals, alloys and semiconductors. Although atomic hydrogen is able to reduce some metal oxides in thermodynamics, the effect of hydrogen on dielectric ceramics has long been neglected since it is generally thought that ceramics are chemically inert near room temperature. To our knowledge, the stability of metal elements in PMN-based ferroelectrics against electroplating has not yet been reported and little is known about the possible reduction process. In the present study, we investigate the resistance degradation of PMZNT during electroplating. The hydrogen effect is discussed and two conduction mechanisms involved in the degradation are proposed.

2 Experimental details

The specimens studied were $0.98Pb(Mg_{1/3}Nb_{2/3})O_3$–$0.01Pb(Zn_{1/3}Nb_{2/3})O_3$–$0.01PbTiO_3$ ceramics (PMZNT). This composition meets the EIA Y5V specification and has been commercialized.[16] The dielectric powder was prepared through a two-stage calcination method suggested by Swartz and Shrout.[1] All raw materials used were of reagent-grade: PbO (Wenzhou Chemical Plant, 99.0% PbO), Nb_2O_5 (Beitong Chemical Plant, 99.5% Nb_2O_5), $Mg(OH)_2 \cdot MgCO_3 \cdot 6H_2O$ [Beijing Chemical Plant, 40.0% MgO in magnesium carbonate (basic)], ZnO (Beijing Chemical Plant, 99.0% ZnO) and TiO_2 (Beijing Yili Fine Chemicals Co. Ltd., 99.0% TiO_2). Two different columbites, $MgNb_2O_6$ and $ZnNb_2O_6$, were firstly prepared at 1000 °C for 4 h through reaction of magnesium carbonate (basic) and zinc oxide with niobium oxide, respectively. Secondly, PbO and TiO_2 were added to the two previously calcined precursors and then ball-milled in water for 24 h, dried and calcined at 800 °C for 2 h. Pellets with a diameter of 1 cm were made by dry pressing under 100 MPa pressure and then buried under the same composition powder in a closed aluminum oxide crucible to minimize the volatilization of PbO. Sintering was carried out at 970 °C for 4 h followed by cooling down in the furnace. Finally, Ag terminations were calcined onto the specimens. The XRD pattern of PMZNT ceramics is presented in Fig. 1. The strongest peaks indicate the formation of the perovskite phase

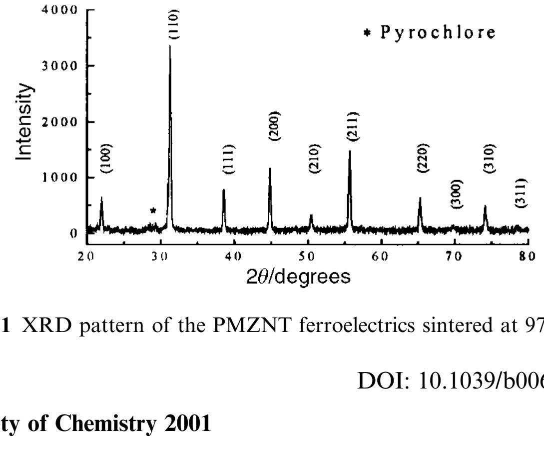

Fig. 1 XRD pattern of the PMZNT ferroelectrics sintered at 970 °C.

J. Mater. Chem., 2001, **11**, 1198–1200 DOI: 10.1039/b006953l

according to JCPDS file 27-1199. As can be seen, the perovskite phase is dominant and the pyrochlore phase can be neglected.

After being cleaned and activated, the specimens were electroplated in a nickel sulfamate-based solution with slight mechanical agitation. Commercial additives were included in the solution to keep the coating smooth and to control the stress in the nickel electrodeposition. The composition of nickel electroplating solution and the processing parameters are listed in Table 1.

XPS analysis was carried out at room temperature on a Perkin Elmer PHI 5300 ESCA/610 SAM using a spherical capacitance analyzer (SCA). Al Kα radiation was adopted as the excitation source, operating at 250 W. Before being sent to the chamber, each sample was cleaned carefully. Vacuum pressure of the instrument chamber was 1×10^{-7} Pa, as read on the panel. The size of detected area was 1×3 mm^2. Measured spectra were decomposed into Gaussian components by a least-squares fitting method. Binding energy was calibrated referenced to the C1s peak (285.0 eV).

3 Results

3.1 Resistivity characteristics

Resistivity changes of the ceramics were examined as a function of electroplating time. As shown in Fig. 2, the resistivity decreased non-linearly with electroplating time. Within the first 2 h of electroplating, there was only a slight resistivity decrease. After that, the resistivity declined rapidly and finally an obvious degradation occurred. We also noted that as the electroplating time increased, the color of the specimens turned darker. For some seriously degraded samples, small parts of the surface near the metal electrodes turned black, or even nickel was electroplated on the ceramics.

3.2 XPS analysis

Fig. 3 gives the Nb 3d and Pb 4f narrow spectra of a blank sample. The binding energies of Nb 3d$_{5/2}$ and Pb 4f$_{7/2}$ were 207.1 and 138.9 eV respectively. The intensity ratios of the two peaks Nb 3d and Pb 4f were *ca.* 3 : 2 and 5 : 3 respectively, while the spin-orbit splittings were 2.8 and 4.9 eV. The spectra were well in accordance with a single Gaussian component. All these values represented the charge states of Nb^{5+} and Pb^{2+}.[17–19]

We examined the spectra of Nb 3d and Pb 4f on samples with different electroplating times. Fig. 4 plots the effect of electroplating on the valence states of Nb and Pb. The dentoid curves represent the original spectra while the smooth curves represent the real components after resolution. As shown in Fig. 4(a), there was only one component in Nb 3d and Pb 4f spectra respectively after the specimen was electroplated for one hour. However, the Nb spectrum became broader after 2 h of electroplating. After resolution, it can be seen that a new component appeared at the lower binding energy side. The spin-orbit splitting was 2.8 eV and intensity ratio of the two peaks also about 3 : 2. The binding energy of the new component was 206.0 eV, which is close to that of Nb^{4+} in the form of NbO$_2$.[17,18] This indicated that a small part of Nb^{5+} was reduced to Nb^{4+} after 2 h of electroplating. The content ratio of Nb^{4+} to Nb^{5+} was *ca.* 1 : 21. After 3 h of electroplating the content of this new component was further enhanced to 1 : 13, as shown in Fig. 4(c) and Table 2. The new component position changed further with electroplating time, and for the specimen undergoing 4.5 h of electroplating, the intensity ratio of Nb^{4+} to Nb^{5+} reached 1.1 : 1. However, no obvious change in the Pb 4f spectra was observed until the sample was electroplated for 4.5 h. A new component appeared at the lower binding energy side near the usual Pb 4f. The binding energy of the new component was 136.9 eV, which was close to that of metallic Pb.[17] The chemical shift was 2.0 eV referenced to Pb^{2+} in the ceramics. These results indicate that not only Nb^{5+}, but also Pb^{2+}, can be reduced to lower valence states during nickel electroplating. They also imply that Nb^{5+} reduction takes place prior to Pb^{2+} reduction.

Table 1 Nickel electroplating process parameters

Nickel sulfamate (g l^{-1})	60
NiCl$_2$ (g l^{-1})	15
Boric acid (g l^{-1})	40
pH	3.8
Temperature (°C)	55
Cathodic current density (A dm^{-2})	1.0

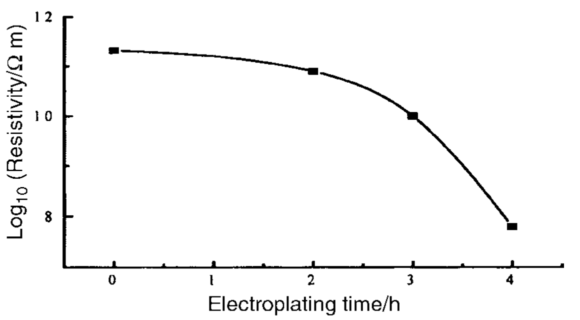

Fig. 2 Resistivity of the ceramics as a function of electroplating time.

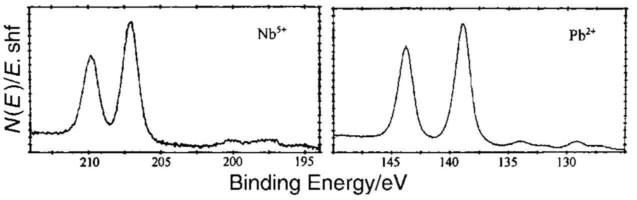

Fig. 3 Nb 3d and Pb 4f X-ray photoelectron spectra of a blank sample.

It is of interest to find the shift of the Nb^{4+} 3d peak. As the

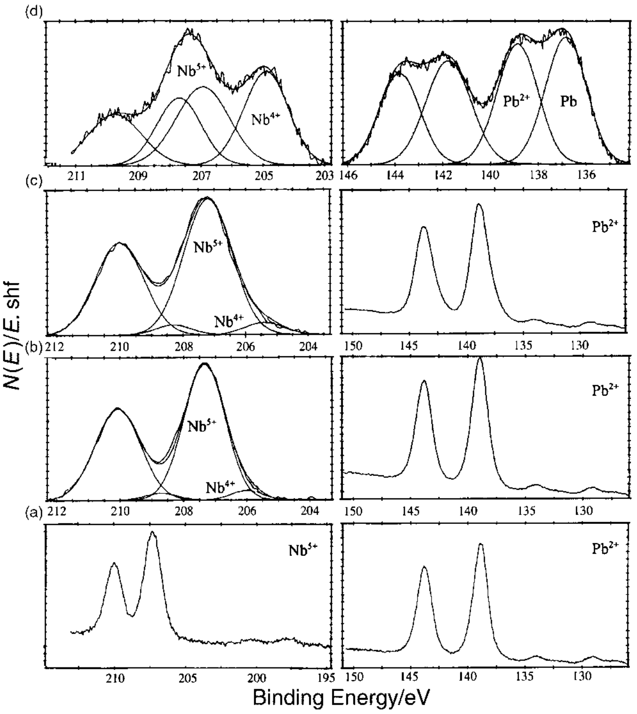

Fig. 4 Nb 3d and Pb 4f X-ray photoelectron spectra of specimens electroplated for different times at 55 °C: (a) 1 h, (b) 2 h, (c) 3 h and (d) 4.5 h.

Table 2 Measured binding energies[a] of Nb and Pb in different samples

Electroplating time/h	Nb^{5+} $3d_{5/2}$	Nb^{4+} $3d_{5/2}$	$Nb^{4+}:Nb^{5+}$ ratio	Pb^{2+} $4f_{7/2}$	Pb $4f_{7/2}$	$Pb:Pb^{2+}$ ratio
Blank specimen	207.1	—	—	138.9	—	—
1	207.1	—	—	138.9	—	—
2	207.2	206.0	1 : 21	138.9	—	—
3	207.2	205.4	1 : 13	138.9	—	—
4.5	207.0	204.9	1.1 : 1	138.9	136.9	1.1 : 1

[a] Binding energies in eV.

Nb^{4+} concentration is increased, the new Nb^{4+} 3d component moves towards the negative side and the interval between Nb^{5+} 3d and Nb^{4+} 3d lines becomes larger, whereas the positions of Nb^{5+} 3d and Pb^{2+} 4f remain unchanged. It may indicate that the concentration of Nb^{4+} had an influence on its chemical shift. This can be attributed to the different 'average' chemical surroundings corresponding to the Nb^{4+} concentration in the Nb^{5+} substrate.

In this study, no significant chemical shift was detected for Zn and Ti, whose contents were very small.

4 Discussion

In this study, the effect of nickel electroplating on resistivity characteristics of the PMN-based ceramics has been studied. The XPS analysis clarified the reduction of the ceramic surface and valence changes of Nb^{5+} and Pb^{2+}. From the results, it can be concluded that the hydrogen generated during electroplating must play an important role. During electroplating, hydrogen atoms are produced and adsorbed on the surface of the cathode. Because of their high activity, they can diffuse along the electrode and subsequently react with the substrate, though most of them finally diffuse into the solution after desorption. In other words, hydrogen reduction led to the resistance deterioration of the ceramics.

Concerning the resistivity changes during electroplating, the reduction of PMZNT ceramics can be divided into three stages. At the first stage, *i.e.* at the beginning of electroplating, there are no detectable Nb^{4+} generated and the resistivity remains almost unchanged accordingly. This can be easily explained as the time limitation. Then as electroplating continues, at the second stage, Nb^{5+} begins to be reduced to lower valence Nb^{4+} and oxygen vacancies are produced according to eqn. (1) (using the defect notations of Kröger–Vink). Oxygen vacancies act as charge carriers, which result in an obvious resistivity decrease. As electroplating time increases further, more and more Nb^{5+} are reduced and $V_O^{\cdot\cdot}$ content is enhanced continuously.

$$2Nb_{Nb} + 5O_O \rightarrow 2Nb'_{Nb} + 4O_O + V_O^{\bullet\bullet} + \frac{1}{2}O_2 \qquad (1)$$

At the third stage, apart from Nb^{5+} reduction, Pb^{2+} reduction to metallic Pb occurs. The ceramic surface begins to be metallized according to eqn. (2), and this, consequently, causes a strong increase in the number of free electrons. Electronic conduction is involved which gives rise to the total conduction. As shown in Fig. 1, the resistivity declines more rapidly.

$$Pb_{Pb} + O_O \rightarrow Pb''_{Pb} + V_O^{\bullet\bullet} + \frac{1}{2}O_2 \qquad (2)$$

In summary, as a result of hydrogen reduction, charge carriers (including oxygen vacancies and free electrons) are created; thereby, insulation resistivity of the ceramic decreases. Nb^{4+} generation may be the reason for the darkening of the ceramic surface since Nb^{4+} is black in the form of NbO_2.

It should be emphasized that Nb^{5+} reduction and Pb^{2+} reduction are not synchronous. To reduce Pb^{2+} needs more electroplating time. Before the samples were electroplated for 3 h, there had existed the resistance decrease. Therefore within the first 3 h of nickel electroplating, the resistance degradation can be just attributed to Nb^{5+} reduction or oxygen vacancy generation. It is suggested that the stability of Nb^{5+} in the ceramic surface should be considered above all with regard to enhancing the reliability of PMN-based ceramics.

5 Conclusions

(1) The XPS results indicate that Nb^{5+} and Pb^{2+} can be reduced to Nb^{4+} and metallic Pb.

(2) The degradation of PMZNT can be attributed to hydrogen generation during electroplating.

(3) Nb^{5+} reduction occurs prior to Pb^{2+} reduction. The resistance degradation at the initial stage of electroplating can be ascribed to Nb^{5+} reduction.

(4) Ionic conduction and electronic conduction are involved in the insulation degradation.

Acknowledgements

The authors are indebted to the financial support from the National Natural Science Foundation of P. R. China (Grant: 59995523).

References

1 S. L. Swartz and T. R. Shrout, *Mater. Res. Bull.*, 1982, **17**, 1245.
2 M. Lejeune and J. P. Boilot, *Mater. Res. Bull.*, 1985, **20**, 493.
3 S. L. Swartz, T. R. Shrout, W. A. Schulze and L. E. Cross, *J. Am. Ceram. Soc.*, 1984, **67**, 311.
4 G. R. Bai, S. K. Streiffer, P. K. Banmann, O. Anciello, K. Ghosh, S. Stemmer, A. Munkholm, C. Thompson, R. A. Rao and C. B. Eom, *Appl. Phys. Lett.*, 2000, **76**, 3106.
5 B. P. Burton, *J. Phys. Chem. Solids*, 2000, **61**, 327.
6 Y. Wang, L. T. Li and Z. L. Gui, *Mater. Lett.*, 1998, **37**, 40.
7 K. Uchino, *Am. Ceram. Soc. Bull.*, 1986, **65**, 647.
8 T. R. Shrout and A. Halliyal, *Am. Ceram. Soc. Bull.*, 1987, **66**, 704.
9 A. W. Travenor, H.-P. S. Li and R. Stevens, *J. Eur. Ceram. Soc.*, 1999, **19**, 1859.
10 O. Furukawa, M. Harata, Y. Yamashita, K. Inagaki and S. Mukaeda, *Jpn. J. Appl. Phys.*, 1987, **26**, 34.
11 A. Moore, *Electronic Production*, 1989, **18**, 25.
12 W. P. Chen, L. T. Li, Y. Wang and Z. L. Gui, *J. Mater. Res.*, 1998, **13**, 1110.
13 D. A. Behm, C. J. Feltz, R. Haynes and S. C. Pinault, *J. Am. Ceram. Soc.*, 1989, **72**, 2279.
14 F. R. Anderson, R. Haynes and S. C. Pinault, *IEEE Transaction on Components, Hybrids, and Manufacturing Technology*, 1989, **12**(4), 609.
15 C. J. Raub, *Plating and Surface Finishing*, 1993, **80**(9), 30–38.
16 Z. L. Gui, Y. Wang and L. T. Li, *Proc. Tenth IEEE Intern. Symp. on Appl. Ferro.*, Aug. 18, 1996, 409–412.
17 John F. Moulder, William F. Stickle, Peter E. Sobol and Kenneth D. Bomben, *Handbook of X-Ray Photoelectron Spectroscopy*, Perkin Elmer Corporation, U.S.A., October, 1992.
18 M. Z. Atashbar, H. T. Sun, B. Gong, W. Wlodarski and R. Lamb, *Thin Solid Films*, 1998, **326**, 238.
19 K. Tabata, T. Choso and Y. Nagasawa, *Surf. Sci.*, 1998, **408**, 137.